Double asynchronous switching control for Takagi-Sugeno fuzzy Markov jump systems via adaptive event-triggered mechanism

Yinghong Zhao, Likui Wang, Xiangpeng Xie, Jiayue Hou, and Hak-Keung Lam

***Abstract*—This article addresses the issue of adaptive event-triggered H_∞ control for Markov jump systems based on Takagi-Sugeno (T-S) fuzzy model. Firstly, a new double asynchronous switching controller is presented to deal with the problem of the mismatch of premise variables and modes between the controller and the plant, which is widespread in real network environment. To further reduce the power consumption of communication, a switching adaptive event-triggered mechanism is adopted to relieve the network transmission pressure while ensuring the control effect. In addition, a new Lyapunov-Krasovskii functional (LKF) is constructed to reduce conservatism by introducing the membership functions (MFs) and time-varying delays information. Meanwhile, the invariant set is estimated to ensure the stability of the system. And the disturbance rejection ability is measured by the optimal H_∞ performance index. Finally, two examples are presented to demonstrate the effectiveness of the proposed approach.**

***Index Terms*—Adaptive event-triggered mechanism, membership functions, double asynchronous switching control, invariant set.**

I. Introduction

IN most practical systems, such as aerospace, economic, and power systems, nonlinearities are prevalent, rendering the challenges of stability analysis and control synthesis. As a crucial tool to investigate nonlinear issues, T-S fuzzy model has attracted increasing attention for its unique advantages [1]. Different from the precise mathematical model required by traditional control theory, T-S fuzzy model is equipped with universal approximate property and can approximate the nonlinear systems effectively [2]–[4]. Recently, the study on T-S fuzzy system has become a hot topic and the relevant achievements mainly focus on sliding mode control [5], observer design [6], stability analysis [7]–[9], etc.

On the other hand, nonlinear systems are frequently subject to unpredictable mutations in their structure and parameters due to environmental degradation, component failures, subsystem interconnection modifications, and other reasons. Markov jump systems (MJSs) provide a suitable framework for modeling these variations, and have wide applications in the fields of communication, robotic manipulators, and aircraft control [10]–[12]. By utilizing the T-S fuzzy approach, nonlinear MJSs can be partitioned into a composite of local linear subsystems, thus effectively addressing nonlinear problems. Consequently, it is significant to further research fuzzy MJSs (FMJSs), and many meaningful topics have been addressed. For instance, the problem of asynchronous sliding mode control for FMJSs with matched uncertainties and external noise was considered in [13]. The finite-time asynchronous control issue for positive hidden FMJSs was addressed in [14]. The problem of event-based asynchronous security control for FMJSs against multi-cyber attacks was investigated in [15].

It is worth mentioning that the transmission of data among sensors, controllers, and actuators via a shared communication network has become an inexorable trend in control theory [16]–[19]. However, the limited communication bandwidth of the network presents challenges to the analysis of FMJSs. In the time-triggered mechanism, the state of the controlled object requires to be transmitted periodically, resulting in an inefficient utilization of communication network resources. To address this issue, the event-triggered mechanism (ETM) is proposed to alleviate the transmission burden [20]–[23]. It should be pointed out that the aforementioned ETM employs a constant threshold, potentially leading to an underutilization of communication resources. To further optimize the transmission bandwidth, a new adaptive ETM (AETM) has attracted significant attention in academic, allowing for the dynamic adjustment of the threshold to adapt system changes [24]–[26]. Hence, it is necessary to research the adaptive event-triggered control for FMJSs, which motivates the present work.

However, due to the influence of sampling behavior and network environment, the premise variables between the controller and the plant are often mismatched, which is usually ignored in the previous work. Thus, it is meaningful to consider the asynchronous premise variables when modeling, analyzing, and controlling FMJSs in the network environment [27]–[29]. On the other hand, the system modes in MJSs are difficult to accurately measure in practical engineering operations since certain technical and financial restrictions. To crack this nut, considerable efforts have been dedicated to study the issue of mode asynchronous, and abundant achievements have been achieved. For example, the asynchronous tracking control issue for discrete time FMJSs was researched in [30]. The problem of asynchronous control for MJSs with

The work was supported in part by the National Natural Science Foundation of China under Grant 62173123, and in part by the Natural Science Foundation of Hebei Province under Grant F2021202045.

Yinghong Zhao and Likui Wang are with the School of Artificial Intelligence, Hebei University of Technology, Tianjin 300401, China (e-mail: zyh_0505@126.com; wlk0228@163.com).

Xiangpeng Xie and Jiayue Hou are with Institute of Advanced Technology Nanjing University of Posts and Telecommunications, Nanjing 210003, China (email: xiexiangpeng1953@163.com; 657794188@qq.com).

Hak-Keung Lam is with the Department of Informatics, King's College London, London WC2R 2LS, U.K. (e-mail: hak-keung.lam@kcl.ac.uk).

Corresponding author: Likui Wang (e-mail: wlk0228@163.com).

actuator saturation was discussed in [31]. Utilizing the hidden Markov model (HMM), the event-triggered-based control for stochastic networked MJSs was considered in [32]. The asynchronous control issue for MJSs under aperiodic denial-of-service attacks was investigated in [33]. Nevertheless, the double asynchronous of modes and premise variables between the controller and the plant in network environments has not been well considered, which is another motivation of this paper.

Note that most of the existing works on FMJSs are based on MFs-independent LKF, which inevitably leads to conservatism. As a unique feature of fuzzy systems, the consideration of MFs in LKF is essential, but the processing of the time derivative of MFs is a challenging subject. For this problem, the bounded time derivative of MFs was proposed in [34]–[36], but it is actually difficult to get. In [7], [8], a switching method was introduced to address the time derivative of MFs and this method relies on the assumption of a finite number of switches. Furthermore, the issue of double asynchronous switching control for FMJSs under network environments has not been researched, and this is a gap we intend to address.

In light of the preceding discussion, we are motivated to investigate the issue of double asynchronous switching control for FMJSs based on AETM. The primary contributions can be stated as follows:

1) Unlike the synchronous or single-asynchronous phenomenon described in the past results, the modes and premise variables between the controller and the plant are mismatched simultaneously. Employing the switching approach, a more general double asynchronous switching controller is presented for the first time.
2) A new mode-dependent switching AETM is designed to economize more transmission resources. Besides, a MFs-dependent LKF containing time delay information is constructed to reduce conservatism. This yields a stability criterion that is more practical and less conservative, as demonstrated in Example 2.
3) The estimation of invariant set is used to ensure the stability and two sets are designed such that any system trajectories starting from the smaller set will remain in the larger set.

Notation: R^n stands for the n-dimensional Euclidean space; $G > 0$ (< 0) signifies that G is symmetric positive (negative); $E\{\cdot\}$ represents the mathematical expectation; $\|\cdot\|$ indicates the Euclidean norm; "$*$" denotes symmetry; $sym(H)$ refers to $H + H^T$; $\mathcal{L}$ represents the weak infinitesimal operator; $diag\{\cdots\}$ represents a block-diagonal matrix; $\mathfrak{k}_{\mathfrak{h}}$ indicates that only the element in $(1, \mathfrak{h})$ is 1, and the others are 0.

II. Problem formulation and preliminaries

Consider the following FMJSs:

Plant Rule i: IF $\wp_1(t)$ is N_{i1}, …, $\wp_g(t)$ is N_{ig}, THEN

$$\begin{cases} \dot{x}(t) = A_{\theta(t)i}x(t) + B_{1\theta(t)i}u(t) + D_{\theta(t)i}w(t), \\ y(t) = C_{\theta(t)i}x(t) + B_{2\theta(t)i}u(t) + E_{\theta(t)i}w(t), \end{cases} \tag{1}$$

where $x(t) \in R^n$, $y(t) \in R^s$, $u(t) \in R^l$, and $w(t) \in R^w$ denote the system state, controlled output, controlled input, and external disturbance, respectively. $\wp_\dagger(t)$ are the premise variables in compact set $\mathbb{C}$, $N_{i\dagger}(i = 1, 2, \ldots, r, \dagger = 1, 2, \ldots, g)$ represent the fuzzy sets with r rules. The matrices within system (1) are predefined and real. $\theta(t) \in \mathcal{N} = \{1, 2, \ldots, N\}$ is a continuous Markov chain. The transition probability (TP) matrix $\Pi_1 = [\pi_{pq}]$ can be expressed as:

$$\Pr\{\theta_{t+\Delta t} = q \,|\theta_t = p\} = \begin{cases} \pi_{pq}\Delta t + o(\Delta t), & p \neq q, \\ 1 + \pi_{pp}\Delta t + o(\Delta t), & p = q, \end{cases} \tag{2}$$

with $\Delta t > 0$ and $\lim\limits_{\Delta t \to 0} \frac{o(\Delta t)}{\Delta t} = 0$, π_{pq} satisfies $\pi_{pq} \geq 0$ with $p \neq q$ and $\pi_{pp} = -\sum_{q=1, q\neq p}^{N} \pi_{pq}$.

Employing the product-fuzzy inference, we can get the MF is $h_i(\wp(t)) = \frac{\prod_{\dagger=1}^{g} \Re_{i\dagger}(\wp_\dagger(t))}{\sum_{i=1}^{r}\prod_{\dagger=1}^{g} \Re_{i\dagger}(\wp_\dagger(t))}$, and $\Re_{i\dagger}(\wp_\dagger(t))$ is the grade of membership of $\wp_\dagger(t)$ in $\Re_{i\dagger}$. Evidently, $h_i(\wp(t)) \geq 0$, $\sum_{i=1}^{r} h_i(\wp(t)) = 1$.

For conciseness, when $\theta(t) = p$, we denote $\sum_{i=1}^{r} h_i Q_{pi}$ as Q_{ph}, where $h_i = h_i(\wp(t))$. The system (1) can be represented as follows:

$$\begin{cases} \dot{x}(t) = A_{ph}x(t) + B_{1ph}u(t) + D_{ph}w(t), \\ y(t) = C_{ph}x(t) + B_{2ph}u(t) + E_{ph}w(t). \end{cases} \tag{3}$$

Assumption 1: The disturbance input $w(t)$ is energy bounded, i.e. $\int_0^t w^T(t)w(t)dt \leq \theta$, where $\theta > 0$ is a given constant.

In this paper, an AETM is established to reduce unnecessary communication consumption and save network resources. Denote $i_k\mathcal{T}(i_k \in N, i_0 = 0)$ as the latest triggered instant with sampling period $\mathcal{T}$, the event-triggering condition can be represented as:

$$\begin{aligned} &(x(i_k\mathcal{T}+l\mathcal{T}) - x(i_k\mathcal{T}))^T\Omega_p(x(i_k\mathcal{T}+l\mathcal{T}) - x(i_k\mathcal{T})) \\ &\geq \delta(t)x^T(i_k\mathcal{T})\Omega_p x(i_k\mathcal{T}), \end{aligned} \tag{4}$$

where Ω_p are positive matrices to be designed. If (4) holds, the present sampled data $x(i_k\mathcal{T} + l\mathcal{T})$ will be sent to the controller as the latest triggered instant $x(i_{k+1}\mathcal{T})$. Define $e_{i_k}(t) = x(i_k\mathcal{T}) - x(i_k\mathcal{T} + l\mathcal{T})$, $\delta(t)$ is a function satisfying

$$\dot{\delta}(t) = \frac{1}{\delta(t)}\left(\frac{1}{\delta(t)} - \delta\right) e_{i_k}^T(t)\Omega_p e_{i_k}(t), \tag{5}$$

where $\delta > 0$ is a pregiven value, $\delta(0) \in (0, 1)$.

Remark 1: Ω_p depends on the system mode, so that the event-triggering condition (4) can be switched accordingly for each Markov jump subsystem, increasing the degree of freedom of feasible solutions. Moreover, unlike the constant threshold employed in [20]–[22], the threshold $\delta(t)$ is dynamically adjusted. When $\delta = \frac{1}{\delta(0)}$ (i.e. $\dot{\delta}(t) = 0$), the AETM will be converted to the traditional event triggering mechanism (TETM) that satisfies the following triggered condition

$$\begin{aligned} &(x(i_k\mathcal{T}+l\mathcal{T}) - x(i_k\mathcal{T}))^T\Omega_p(x(i_k\mathcal{T}+l\mathcal{T}) - x(i_k\mathcal{T})) \\ &\geq \delta^* x^T(i_k\mathcal{T})\Omega_p x(i_k\mathcal{T}), \end{aligned} \tag{6}$$

where $\delta^* \in [0, 1)$ is a preset constant.

Assuming the delay of the kth triggering instant is d_k, the data packet will reach the zero-order hold (ZOH) at instants $t_k = i_k\mathcal{T} + d_k$. Therefore, the time interval

$[i_k\mathcal{T}+d_k, i_{k+1}\mathcal{T}+d_{k+1})$ can be decomposed into the subintervals as follows:

$$[i_k\mathcal{T}+d_k, i_{k+1}\mathcal{T}+d_{k+1}) = \bigcup_{\mathfrak{M}=0}^{\mathrm{j}_k} \mathfrak{A}_{\mathfrak{M}}, \tag{7}$$

with

$$\begin{cases} \mathfrak{A}_0 = \left[i_k\mathcal{T}+d_k, i_k\mathcal{T}+\mathcal{T}+\bar{d}\right), \\ \mathfrak{A}_{\mathrm{j}} = \left[i_k\mathcal{T}+\mathrm{j}\mathcal{T}+\bar{d}, i_k\mathcal{T}+(\mathrm{j}+1)\mathcal{T}+\bar{d}\right), \\ \mathfrak{A}_{\mathrm{j}_k} = \left[i_k\mathcal{T}+\mathrm{j}_k\mathcal{T}+\bar{d}, i_{k+1}\mathcal{T}+d_{k+1}\right), \end{cases} \tag{8}$$

where $\mathrm{j} = 1, 2, \ldots, \mathrm{j}_k - 1$. Defining $d(t) = t - i_k\mathcal{T} - l\mathcal{T}$ with $\dot{d}(t) = 1$, we have $0 \le d(t) \le \bar{d} + \mathcal{T} = d$. The transmitted state $x(i_k\mathcal{T})$ is estimated as:

$$x(i_k\mathcal{T}) = x(t-d(t)) + e_{i_k}(t). \tag{9}$$

For simplicity, we replace $u(t)$ with u, and the following double asynchronous controller is applied:

Controller Rule j: IF $\wp_1(i_k\mathcal{T})$ is N_{j1}, …, $\wp_g(i_k\mathcal{T})$ is N_{jg}, THEN

$$u = K_{o(t)j}x(i_k\mathcal{T}), \tag{10}$$

where $o(t) \in \mathcal{O} = \{1, 2, \ldots, O\}$ is a stochastic variable to represent the controller mode, which is governed by a conditional probability (CP) matrix $\Pi_2 = [\sigma_{p\vartheta}]$ with

$$\Pr\{o(t) = \vartheta \,|\theta(t) = p\} = \sigma_{p\vartheta}, \tag{11}$$

where $\sigma_{p\vartheta} \in [0,1]$, $\sum_{\vartheta=1}^{O}\sigma_{p\vartheta} = 1$.

Remark 2: Due to various adverse factors such as time delays, information loss, and financial constraints, system-controller asynchrony is inevitable in practical engineering. For this problem, HMM $(\theta(t), o(t), \Pi_1, \Pi_2)$ is used in this paper to express the asynchrony between the controller and the plant. Suppose the signals of the HMM are not completely observable. In such cases, the observable ones can be applied to estimate the hidden modes of the system, which can be obtained from the TP matrix Π_1 and the CP matrix Π_2.

Overall, the controller can be represented as

$$u = \sum_{j=1}^{r} h_j(\wp(i_k\mathcal{T}))K_{\vartheta j}x(i_k\mathcal{T}). \tag{12}$$

Inspired by [27], the asynchronous constraints of the MFs are expressed as

$$\begin{cases} h_j(\wp(i_k\mathcal{T})) = \varphi_j h_j(\wp(t)), \\ |h_j(\wp(i_k\mathcal{T})) - h_j(\wp(t))| \le \lambda_j, \end{cases} \tag{13}$$

where $\varphi_j > 0$, $\lambda_j \ge 0$, $j = 1, 2, ..., r$.

From (13), we have the following inequality:

$$\kappa_1^j = 1 - \frac{\lambda_j}{h_j(\wp(t))} \le \varphi_j \le 1 + \frac{\lambda_j}{h_j(\wp(t))} = \kappa_2^j, \tag{14}$$

where κ_1^j and κ_2^j are the lower and upper bounds of φ_j. Then, we have

$$\frac{1}{\kappa} \le \frac{\varphi_i}{\varphi_j} \le \kappa, \kappa \ge 1, \tag{15}$$

with $\kappa = \frac{\kappa_2}{\kappa_1}$, $\kappa_2 = \max\left\{\kappa_2^j\right\}$, $\kappa_1 = \min\left\{\kappa_1^j\right\}$.

Remark 3: Obviously, the consideration of AETM leads to a mismatch of premise variables between system (3) and controller (12). Hence, the asynchronous constraint (13) is introduced in this paper to address this issue. In particular, when $\kappa = 1$, we have $\max\left\{\kappa_2^j\right\} = \min\left\{\kappa_1^j\right\}$, i.e. $\varphi_j = 1$, the synchronous premise variables are obtained, which is generally considered in the existing results [7]–[9].

Combining (9), (12), and (13), the system (3) is rewritten as follows:

$$\begin{cases} \dot{x}(t) = A_{ph}x(t) + B_{1p\vartheta hh}x(t-d(t)) \\ \qquad\quad + B_{1p\vartheta hh}e_{i_k}(t) + D_{ph}w(t), \\ y(t) = C_{ph}x(t) + B_{2p\vartheta hh}x(t-d(t)) \\ \qquad\quad + B_{2p\vartheta hh}e_{i_k}(t) + E_{ph}w(t), \\ x(t) = \phi(t), t \in [-d, 0], \end{cases} \tag{16}$$

with $B_{\iota p\vartheta hh} = \sum_{i=1}^{r}\sum_{j=1}^{r}\varphi_j h_i h_j B_{\iota pi}K_{\vartheta j}$, $\iota = 1, 2$.

Consider a new LKF that depends on both MFs and modes: $V(x_t) = x^T(t)Q_{ph}x(t)$. A switching method is applied to ensure $\dot{Q}_{ph} < 0$. Based on (13), the time derivative of Q_{ph} in mode p is

$$\dot{Q}_{ph} = \sum_{j=1}^{r}\dot{h}_j Q_{pj} = \sum_{k=1}^{r-1}\dot{h}_k(Q_{pk} - Q_{pr}), \tag{17}$$

where $\dot{h}_k$ represents the time derivative of MFs, which are negative or positive. The switching method is designed as follows:

$$\begin{cases} \text{if } \dot{h}_k < 0, \text{ then } Q_{pk} - Q_{pr} > 0, \\ \text{if } \dot{h}_k \ge 0, \text{ then } Q_{pk} - Q_{pr} \le 0. \end{cases} \tag{18}$$

There are 2^{r-1} constraints for each mode in (18). Define $\mathcal{H}_\chi$ as the potential permutations of $\dot{h}_k$, $\mathfrak{G}_{\chi(p)}$ as the potential constraints of Q_{pj}, $\chi = 1, 2, \ldots, 2^{r-1}$, $p \in \mathcal{N}$, then (18) can be presented as

$$\text{if } \mathcal{H}_\chi, \text{then } \mathfrak{G}_{\chi(p)}. \tag{19}$$

Remark 4: The overall structural illustration of FMJSs is depicted in Figure 1. Synthesizing the above two asynchronous phenomena, according to (19), a fuzzy-model-based double asynchronous switching controller is firstly presented in this paper. For different $\mathcal{H}_\chi$ and $\mathfrak{G}_{\chi(p)}$, the corresponding controller is:

$$u^\chi = \sum_{j=1}^{r} h_j(\wp(i_k\mathcal{T}))K_{\vartheta j}^\chi x(i_k\mathcal{T}). \tag{20}$$

And the adapt event-triggering condition (4) is also changed to the following switching form:

$$\begin{aligned} &(x(i_k\mathcal{T}+l\mathcal{T}) - x(i_k\mathcal{T}))^T\Omega_p^\chi(x(i_k\mathcal{T}+l\mathcal{T}) - x(i_k\mathcal{T})) \\ &\ge \delta(t)x^T(i_k\mathcal{T})\Omega_p^\chi x(i_k\mathcal{T}). \end{aligned} \tag{21}$$

Definition 1: *[37]* The system (16) is stochastically stable, if the following inequality holds for any initial condition $x(0) \in R^n$ and mode $\theta(0) \in \mathcal{N}$:

$$E\left\{\int_0^\infty \|x(\alpha)\|^2 d\alpha \,|x(0), \theta(0)\right\} < \infty.$$

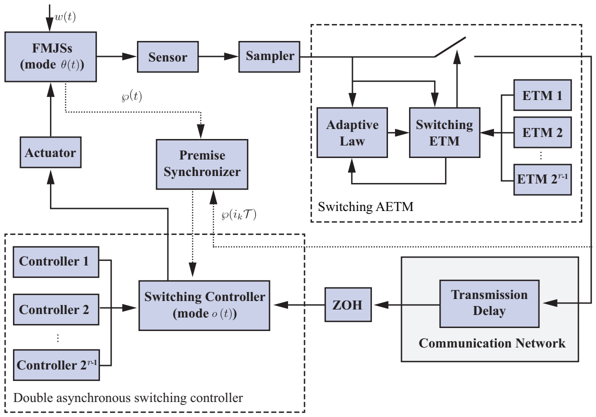

Fig. 1. The framework of FMJSs under double asynchronous switching controller based on AETM.

III. Main results

To facilitate convenient analysis, the notations are presented as follows:

$$
\begin{aligned}
\varsigma_1(t) &= \frac{1}{d}\int_{t-d}^{t} x(\alpha)d\alpha, \varsigma_2(t) = \frac{1}{d-d(t)}\int_{t-d}^{t-d(t)} x(\alpha)d\alpha,\\
\varsigma_3(t) &= \frac{1}{d(t)}\int_{t-d(t)}^{t} x(\alpha)d\alpha, \varsigma_4(t) = \frac{1}{d^2}\int_{t-d}^{t}\int_{\beta}^{t} x(\alpha)d\alpha d\beta,\\
\varsigma(t) &= \left[\begin{array}{cccc} x(t) & \dot{x}(t) & x(t-d) & x(t-d(t)) \end{array}\right],\\
\xi(t) &= col\left\{\varsigma(t), \varsigma_1(t), \varsigma_2(t), \varsigma_3(t), \varsigma_4(t), e_{i_k}(t), w(t)\right\},\\
\rho(t) &= col\left\{x(t), d\varsigma_1(t)\right\}, \eta_1(t) = col\left\{x(t), \varsigma_2(t)\right\},\\
\eta_2(t) &= col\left\{x(t), \varsigma_3(t)\right\}, \Gamma_1 = col\left\{e_1, de_5\right\},\\
\Gamma_2 &= col\left\{e_2, e_1 - e_3\right\}, \Gamma_3 = col\left\{\aleph_1, \aleph_2, \aleph_3, \aleph_4\right\},\\
\Gamma_4 &= col\left\{\aleph_5, \aleph_6\right\}, \Gamma_5 = col\left\{e_1, e_6\right\},\\
\Gamma_6 &= col\left\{(d-d(t))e_2, e_6 - e_3\right\}, \Gamma_7 = col\left\{e_1, e_7\right\},\\
\Gamma_8 &= col\left\{d(t)e_2, e_1 - e_7\right\}, \aleph_1 = e_4 - e_3,\\
\aleph_2 &= e_4 + e_3 - 2e_6, \aleph_3 = e_1 - e_4, \aleph_4 = e_1 + e_4 - 2e_7,\\
\aleph_5 &= e_1 - e_5, \aleph_6 = e_1 + 2e_5 - 6e_8,\\
e_{\mathfrak{r}} &= \left[0_{n\times(\mathfrak{r}-1)n}, I_n, 0_{n\times((9-\mathfrak{r})n+w)}\right],\\
e_{10} &= \left[0_{w\times 9n}, I_w\right], \mathfrak{r} = 1, 2, \ldots, 9.
\end{aligned}
$$

Theorem 1: Giving constants $\kappa \geq 1$, $d \geq 0$, $\delta > 0$, $\gamma > 0$, and $\theta > 0$, the trajectories of system (16) starting from $\mathcal{D}_1$ will stay in $\mathcal{D}_2$ for time $t > d$

$$
\begin{aligned}
\mathcal{D}_1 &:= \left\{\phi(t) : \sum_{\varpi=1}^{5} V_{\varpi}(x_t)\,|_{t=0} \leq 1\right\},\\
\mathcal{D}_2 &:= \left\{x(t) : \sum_{\varpi=1}^{5} V_{\varpi}(x_t) \leq 1 + \theta\gamma^2\right\},
\end{aligned}
$$

if there exist positive definite matrices Q_{pj}, $S_{bj} \in R^{2n\times 2n}$, R_{1pj}, R_{cj}, $\Omega_p \in R^{n\times n}$, matrices U_{gj}, $F \in R^{n\times n}$, such that (19) and the following inequalities hold for $p \in \mathcal{N}$, $\vartheta \in \mathcal{O}$, $\mathcal{K} \in \left\{\kappa, \frac{1}{\kappa}\right\}$, $b = 1, 2$, $c = 1, 2, 3$, $g = 1, 2, 3, 4$

$$
\left[\begin{array}{cc} \Theta^2_{p\vartheta ii} & \Theta^{4T}_{p\vartheta ii} \\ * & -I \end{array}\right] < 0, \tag{22}
$$

$$
\left[\begin{array}{ccc} \Theta^2_{p\vartheta ij} + \mathcal{K}\Theta^2_{p\vartheta ji} & \Theta^{4T}_{p\vartheta ij} & \sqrt{\kappa}\Theta^{4T}_{p\vartheta ji} \\ * & -I & 0 \\ * & * & -I \end{array}\right] < 0, \tag{23}
$$

$$
\sum_{q=1}^{N} \pi_{pq} R_{1qj} - R_{1j} \leq 0, \tag{24}
$$

$$
\Psi_j \geq 0, \tag{25}
$$

where

$$
\begin{aligned}
\Psi_j &= \left[\begin{array}{cc} \bar{R}_{2j} & \bar{U}_j \\ * & \bar{R}_{2j} \end{array}\right], \bar{U}_j = \left[\begin{array}{cc} U_{1j} & U_{2j} \\ U_{3j} & U_{4j} \end{array}\right],\\
\Theta^2_{p\vartheta ij} &= \Theta^1_{p\vartheta ij} - \gamma^2 e_{10}^T e_{10},\\
\Theta^1_{p\vartheta ij} &= sym(\Gamma_1^T Q_{pj}\Gamma_2 + \mathcal{F}_0^T \Im_{p\vartheta ij}) + \Gamma_1^T \sum_{q=1}^{N} \pi_{pq} Q_{qj}\Gamma_1\\
&\quad + e_1^T(R_{1pj} + dR_{1j})e_1 - e_3^T R_{1pj} e_3 + e_2^T(d^2 R_{2j}\\
&\quad + \frac{1}{2}d^2 R_{3j})e_2 - \Gamma_5^T S_{1j}\Gamma_5 + 2\Gamma_5^T S_{1j}\Gamma_6 + \Gamma_7^T S_{2j}\Gamma_7\\
&\quad + 2\Gamma_7^T S_{2j}\Gamma_8 + e_4^T\Omega_p e_4 + e_9^T(\Omega_p - \delta\Omega_p)e_9\\
&\quad + 2e_4^T\Omega_p e_9 - \Gamma_3^T\Psi_j\Gamma_3 - \Gamma_4^T\bar{R}_{3j}\Gamma_4,\\
\mathcal{F}_0 &= F^T e_1 + F^T e_2, \Im_{p\vartheta ij} = -e_2 + A_{pi}e_1\\
&\quad + \sum_{\vartheta=1}^{O} \sigma_{p\vartheta} B_{1pi} K_{\vartheta j}(e_4 + e_9) + D_{pi}e_{10},\\
\Theta^4_{p\vartheta ij} &= col\left\{\sqrt{\sigma_{p1}}\mathcal{Y}_{p1ij}, \sqrt{\sigma_{p2}}\mathcal{Y}_{p2ij}, \ldots, \sqrt{\sigma_{pO}}\mathcal{Y}_{pOij}\right\},\\
\mathcal{Y}_{p\vartheta ij} &= C_{pi}e_1 + B_{2pi}K_{\vartheta j}(e_4 + e_9) + E_{pi}e_{10},\\
\bar{R}_{2j} &= diag\left\{R_{2j}, 3R_{2j}\right\}, \bar{R}_{3j} = diag\left\{2R_{3j}, 4R_{3j}\right\}.
\end{aligned}
$$

Proof: The MFs-dependent LKF is chosen as:

$$
V(x_t) = \sum_{\varpi=1}^{5} V_{\varpi}(x_t), \tag{26}
$$

where

$$
\begin{aligned}
V_1(x_t) &= \rho^T(t) Q_{ph}\rho(t),\\
V_2(x_t) &= \int_{t-d}^{t} x^T(\alpha) R_{1ph} x(\alpha)d\alpha\\
&\quad + \int_{-d}^{0}\int_{t+\beta}^{t} x^T(\alpha) R_{1h} x(\alpha)d\alpha d\beta,\\
V_3(x_t) &= d\int_{-d}^{0}\int_{t+\beta}^{t} \dot{x}^T(\alpha) R_{2h}\dot{x}(\alpha)d\alpha d\beta\\
&\quad + \int_{t-d}^{t}\int_{\gamma}^{t}\int_{\beta}^{t} \dot{x}^T(\alpha) R_{3h}\dot{x}(\alpha)d\alpha d\beta d\gamma,\\
V_4(x_t) &= (d - d(t))\eta_1^T(t) S_{1h}\eta_1(t) + d(t)\eta_2^T(t) S_{2h}\eta_2(t),\\
V_5(x_t) &= \frac{1}{2}\delta^2(t),\\
Q_{ph} &= \left[\begin{array}{cc} Q_{1ph} & Q_{2ph} \\ * & Q_{4ph} \end{array}\right], S_{bh} = \left[\begin{array}{cc} S^1_{bh} & S^2_{bh} \\ * & S^4_{bh} \end{array}\right].
\end{aligned}
$$

Then, we have

$$
\mathcal{L}V(x_t) = \mathcal{L}V^1(x_t) + \mathcal{L}V^2(x_t), \tag{27}
$$

where

$$\mathcal{L}V^1(x_t) = \xi^T(t)\{2\,\Gamma_1^T Q_{ph}\Gamma_2 + \Gamma_1^T\sum_{q=1}^{N}\pi_{pq}Q_{qh}\Gamma_1$$
$$+ e_1^T(R_{1ph}+dR_{1h})e_1 - e_3^T R_{1ph}e_3 + e_2^T(d^2R_{2h}$$
$$+ \frac{1}{2}d^2R_{3h})e_2 - \Gamma_5^T S_{1h}\Gamma_5 + 2\Gamma_5^T S_{1h}\Gamma_6$$
$$+\Gamma_7^T S_{2h}\Gamma_7 + 2\Gamma_7^T S_{2h}\Gamma_8\}\,\xi(t) + \left(\frac{1}{\delta(t)}-\delta\right)$$
$$\times e_{i_k}^T(t)\Omega_p e_{i_k}(t) + \int_{t-d}^{t} x^T(\alpha)(\sum_{q=1}^{N}\pi_{pq}R_{1qh}$$
$$- R_{1h})x(\alpha)d\alpha - d\int_{t-d}^{t}\dot{x}^T(\alpha)R_{2h}\dot{x}(\alpha)d\alpha$$
$$- \int_{t-d}^{t}\int_{\beta}^{t}\dot{x}^T(\alpha)R_{3h}\dot{x}(\alpha)d\alpha d\beta,$$

$$\mathcal{L}V^2(x_t) = \rho^T(t)\dot{Q}_{ph}\rho(t) + (d-d(t))\eta_1^T(t)\dot{S}_{1h}\eta_1(t)$$
$$+ d(t)\eta_2^T(t)\dot{S}_{2h}\eta_2(t) + \int_{t-d}^{t}x^T(\alpha)\dot{R}_{1ph}x(\alpha)d\alpha$$
$$+ \int_{-d}^{0}\int_{t+\beta}^{t}x^T(\alpha)\dot{R}_{1h}x(\alpha)d\alpha d\beta$$
$$+ d\int_{-d}^{0}\int_{t+\beta}^{t}\dot{x}^T(\alpha)\dot{R}_{2h}\dot{x}(\alpha)d\alpha d\beta$$
$$+ \int_{t-d}^{t}\int_{\gamma}^{t}\int_{\beta}^{t}\dot{x}^T(\alpha)\dot{R}_{3h}\dot{x}(\alpha)d\alpha d\beta d\gamma.$$

According to (4) and (5), it has

$$\left(\frac{1}{\delta(t)}-\delta\right)e_{i_k}^T(t)\Omega_p e_{i_k}(t) \le \xi^T(t)(e_4^T\Omega_p e_4 + e_9^T(\Omega_p-\delta\Omega_p)e_9 + 2e_4^T\Omega_p e_9)\xi(t). \tag{28}$$

Based on (13) and system (16), for any invertible matrix $F \in R^{n\times n}$, since $\sum_{\vartheta=1}^{O}\sigma_{p\vartheta}=1$, we have

$$\begin{aligned} 0 &= 2\xi^T(t)\left\{(e_1^TF + e_2^TF)\sum_{\vartheta=1}^{O}\sigma_{p\vartheta}(-e_2 + A_{ph}e_1\right. \\ &\quad \left. + B_{1p\vartheta hh}(e_4+e_9) + D_{ph}e_{10})\right\}\xi(t) \\ &= \xi^T(t)\sum_{i=1}^{r}\sum_{j=1}^{r}\varphi_j h_i h_j\, sym(\mathcal{F}_0^T\Im_{p\vartheta ij})\xi(t), \end{aligned} \tag{29}$$

where $\mathcal{F}_0$ and $\Im_{p\vartheta ij}$ are defined in Theorem 1.

Combining (19), (27)-(29), and applying the methods in [39] and [40] to address terms $-d\int_{t-d}^{t}\dot{x}^T(\alpha)R_{2h}\dot{x}(\alpha)d\alpha$ and $-\int_{t-d}^{t}\int_{\beta}^{t}\dot{x}^T(\alpha)R_{3h}\dot{x}(\alpha)d\alpha d\beta$, we can obtain

$$\mathcal{L}V(x_t) \le \xi^T(t)\sum_{i=1}^{r}\sum_{j=1}^{r}\varphi_j h_i h_j\Theta^1_{p\vartheta ij}\xi(t). \tag{30}$$

The subsequent H_∞ performance function $\mathcal{J}$ is considered:

$$\begin{aligned} \mathcal{J} &= \mathcal{L}V(x_t) + y^T(t)y(t) - \gamma^2 w^T(t)w(t) \\ &\le \xi^T(t)\left\{\sum_{i=1}^{r}\varphi_i h_i^2(\Theta^2_{p\vartheta ii}+\Theta^3_{p\vartheta ii}) + \sum_{i=1}^{r-1}\sum_{j>i}^{r}\varphi_j h_i h_j\right. \\ &\quad \left.\times(\Theta^2_{p\vartheta ij} + \frac{\varphi_i}{\varphi_j}\Theta^2_{p\vartheta ji} + \Theta^3_{p\vartheta ij} + \frac{\varphi_i}{\varphi_j}\Theta^3_{p\vartheta ji})\right\}\xi(t), \end{aligned}$$

with $\Theta^3_{p\vartheta ij} = \sum_{\vartheta=1}^{O}\sigma_{p\vartheta}\mathcal{Y}^T_{p\vartheta ij}\mathcal{Y}_{p\vartheta ij}$.

On account of Schur complement, (22) and (23) imply that

$$\Theta^2_{p\vartheta ii} + \Theta^3_{p\vartheta ii} < 0, \tag{31}$$

$$\Theta^2_{p\vartheta ij} + \kappa\Theta^2_{p\vartheta ji} + \Theta^3_{p\vartheta ij} + \kappa\Theta^3_{p\vartheta ji} < 0, \tag{32}$$

$$\Theta^2_{p\vartheta ij} + \frac{1}{\kappa}\Theta^2_{p\vartheta ji} + \Theta^3_{p\vartheta ij} + \kappa\Theta^3_{p\vartheta ji} < 0. \tag{33}$$

Defining $\beta_1 = (\kappa - \frac{\varphi_i}{\varphi_j})\Big/(\kappa - \frac{1}{\kappa})$, $\beta_2 = (\frac{\varphi_i}{\varphi_j} - \frac{1}{\kappa})\Big/(\kappa - \frac{1}{\kappa})$, from $(\kappa - \frac{\varphi_i}{\varphi_j})\Theta^3_{p\vartheta ji} > 0$, (32) and (33) can be rewritten as

$$\begin{aligned} 0 &> \beta_1(\Theta^2_{p\vartheta ij} + \frac{1}{\kappa}\Theta^2_{p\vartheta ji} + \Theta^3_{p\vartheta ij} + \frac{\varphi_i}{\varphi_j}\Theta^3_{p\vartheta ji}) \\ &\quad + \beta_2(\Theta^2_{p\vartheta ij} + \kappa\Theta^2_{p\vartheta ji} + \Theta^3_{p\vartheta ij} + \frac{\varphi_i}{\varphi_j}\Theta^3_{p\vartheta ji}), \end{aligned} \tag{34}$$

which yields

$$\Theta^2_{p\vartheta ij} + \frac{\varphi_i}{\varphi_j}\Theta^2_{p\vartheta ji} + \Theta^3_{p\vartheta ij} + \frac{\varphi_i}{\varphi_j}\Theta^3_{p\vartheta ji} < 0. \tag{35}$$

According to (31) and (35), it follows that $\mathcal{J} < 0$, i.e. $V(x_t) < V(x_0) + \gamma^2\int_0^t w^T(t)w(t)dt$. From Assumption 1, we have $V(x_t) < 1 + \theta\gamma^2$. Moreover, when $w(t)=0$, we can easily get $\mathcal{L}V(x_t) \le -\eta x^T(t)x(t)$. Based on Definition 1, system (16) is stochastically stable with H_∞ performance level γ, and the trajectories will start from $\mathcal{D}_1$ and stay in $\mathcal{D}_2$ for time $t > d$. ■

Remark 5: A MFs-dependent LKF with two delay-product-type (DPT) terms is designed in this paper. Unlike the LKF proposed in [22], [24], [25], this LKF has a more general form, and the information of modes, MFs, and time-varying delays are included simultaneously, which is more in line with the model of FMJSs. Besides, the introduction of DPT terms will relax the constraints in some locations and include more time-varying delay information. Therefore, the LKF presented in this paper provides a comprehensive framework for analyzing the stochastic stability and H_∞ performance of FMJSs, which is less conservative than other methods.

The set $\mathcal{D}_1$ is highly complex and difficult to measure precisely because of the presence of integral terms and the derivative of the initial state ($\dot{\phi}(t)$). To estimate the local stabilization region, we assume that $\phi(t)$ and $\dot{\phi}(t)$ are smooth within the interval $[-d,0]$, and for any $t_1, t_2 \in [-d,0]$, we have $\phi(t_1) \le \dot{\phi}(t) \le \phi(t_2)$. Thus, we can obtain $\dot{\phi}(t) = \sum_{\iota=1}^{2}\lambda_\iota(t)\phi(t_\iota)$ with $0 \le \lambda_\iota(t) \le 1$, $\sum_{\iota=1}^{2}\lambda_\iota(t)=1$. Then, it follows that $\dot{\phi}^T(\alpha)R_{\mathfrak{s}h(0)}\dot{\phi}(\alpha) \le \sum_{\iota=1}^{2}\lambda_\iota(\alpha)\phi^{\iota\iota}_{\mathfrak{s}}$, where $\phi^{\iota\iota}_{\mathfrak{s}} = \phi^T(t_\iota)R_{\mathfrak{s}h(0)}\phi(t_\iota)$, $\iota=1,2$, $\mathfrak{s}=2,3$.

Letting $\phi^T(\mathfrak{w})R_{1ph(0)}\phi(\mathfrak{w}) = \bar{\Re}_{1ph(0)}$, $\phi^T(\mathfrak{w})R_{ch(0)}\phi(\mathfrak{w}) = \bar{\Re}_{ch(0)}$ $(c=1,2,3)$, we can obtain

$$V_2(x_t)\,|_{t=0} \le d\max_{-d\le\mathfrak{w}\le0}(\bar{\Re}_{1ph(0)}) + \frac{1}{2}d^2\max_{-d\le\mathfrak{w}\le0}(\bar{\Re}_{1h(0)}),$$

$$\begin{aligned} V_3(x_t)\,|_{t=0} &\le d\int_{-d}^{0}\int_{\beta}^{0}\sum_{\iota=1}^{2}\lambda_\iota(\alpha)\phi_2^{\iota\iota}d\alpha d\beta \\ &\quad + \int_{-d}^{0}\int_{\gamma}^{0}\int_{\beta}^{0}\sum_{\iota=1}^{2}\lambda_\iota(\alpha)\phi_3^{\iota\iota}d\alpha d\beta d\gamma \\ &\le \frac{1}{2}d^3\max_{-d\le\mathfrak{w}\le0}(\bar{\Re}_{2h(0)}) + \frac{1}{6}d^3\max_{-d\le\mathfrak{w}\le0}(\bar{\Re}_{3h(0)}). \end{aligned}$$

Supposing $Q_{2ph(0)} = Q^T_{2ph(0)} \geq 0$, $S^2_{bh(0)} = S^{2T}_{bh(0)} \geq 0\,(b = 1,2)$, letting $\mathfrak{F}_1 = \int_{-d}^{0}\phi(\alpha)d\alpha$, $\mathfrak{F}_2 = \frac{1}{d-d(0)}\int_{-d}^{-d(0)}\phi(\alpha)d\alpha$, $\mathfrak{F}_3 = \frac{1}{d(0)}\int_{-d(0)}^{0}\phi(\alpha)d\alpha$, we have

$$
\begin{aligned}
V_1(x_t)\,|_{t=0} &\leq \phi^T(0)\mathcal{Z}_{1ph(0)}\phi(0) + \mathfrak{F}_1^T\mathcal{Z}_{2ph(0)}\mathfrak{F}_1 \\
&\leq \max_{-d\leq\mathfrak{w}\leq 0}(\mathfrak{P}_{1ph(0)}) + d^2\max_{-d\leq\mathfrak{w}\leq 0}(\mathfrak{P}_{2ph(0)}), \\
V_4(x_t)\,|_{t=0} &\leq d\left\{\phi^T(0)\mathcal{Z}_{3h(0)}\phi(0) + \mathfrak{F}_2^T\mathcal{Z}_{4h(0)}\mathfrak{F}_2 \right.\\
&\quad \left. + \mathfrak{F}_3^T\mathcal{Z}_{5h(0)}\mathfrak{F}_3\right\} \\
&\leq d\max_{-d\leq\mathfrak{w}\leq 0}(\mathfrak{P}_{3h(0)}) + d\max_{-d\leq\mathfrak{w}\leq 0}(\mathfrak{P}_{4h(0)}) \\
&\quad + d\max_{-d\leq\mathfrak{w}\leq 0}(\mathfrak{P}_{5h(0)}), \\
\mathfrak{P}_{\mathfrak{e}(p)h(0)} &= \phi^T(\mathfrak{w})\mathcal{Z}_{\mathfrak{e}(p)h(0)}\phi(\mathfrak{w}), \mathfrak{e} = 1,2,3,4,5,
\end{aligned}
$$

where

$$
\begin{aligned}
&\mathcal{Z}_{1ph(0)} = Q_{1ph(0)} + Q_{2ph(0)}, \mathcal{Z}_{2ph(0)} = Q_{2ph(0)} + Q_{4ph(0)}, \\
&\mathcal{Z}_{3h(0)} = S^1_{1h(0)} + S^2_{1h(0)} + S^1_{2h(0)} + S^2_{2h(0)}, \\
&\mathcal{Z}_{4h(0)} = S^2_{1h(0)} + S^4_{1h(0)}, \mathcal{Z}_{5h(0)} = S^2_{2h(0)} + S^4_{2h(0)}.
\end{aligned}
$$

From $\delta(0) \in (0,1)$, we have $V_5(x_t)\,|_{t=0} = \frac{1}{2}\delta^2(0) \leq \frac{1}{2}$. Therefore, combining the above calculations of $V_1(x_t) - V_5(x_t)$, for positive definite matrix $\mathfrak{S}_{pj}$, consider the following constraint such that the sum of all partial matrices is less than $\mathfrak{S}_{pj}$, i.e.

$$
\begin{aligned}
\mathfrak{S}_{pj} \geq & \frac{1}{2}(d^3R_{2j} + d^2R_{1j} + 1) + \frac{1}{6}d^3R_{3j} + dR_{1pj} + d^2(Q_{2pj} \\
& + Q_{4pj}) + \sum_{b=1}^{2}Q_{bpj} + d\sum_{b=1}^{2}(S^1_{bj} + 2S^2_{bj} + S^4_{bj}), \quad (36)
\end{aligned}
$$

we can obtain the estimation of $\mathcal{D}_1$

$$
\bar{\mathcal{D}}_1 := \left\{\phi(t) : \phi^T(\mathfrak{w})\mathfrak{S}_{ph(0)}\phi(\mathfrak{w}) \leq 1, \forall\mathfrak{w} \in [-d, 0]\right\}. \quad (37)
$$

Similarly, the estimation of $\mathcal{D}_2$ is

$$
\bar{\mathcal{D}}_2 := \left\{x(t) : x^T(t)\mathfrak{S}_{ph(0)}x(t) \leq 1 + \theta\gamma^2\right\}. \quad (38)
$$

Remark 6: It should be pointed out that $\bar{\mathcal{D}}_2$ must be contained in the compact set $\mathbb{C} = \bigcap_{\mathfrak{h}}\left\{x(t) : |\mathfrak{k}_{\mathfrak{h}}x(t)| \leq \beta_{\mathfrak{h}}\right\}, \mathfrak{h} = 1,2,\ldots,n$. According to the Lagrange multiplier method, this constraint means, any t satisfying $\mathfrak{k}_{\mathfrak{h}}x(t) = \pm\beta_{\mathfrak{h}}$, we have $x^T(t)\mathfrak{S}_{pj}x(t) \geq 1 + \theta\gamma^2$, i.e.

$$
\min\left\{x^T(t)\mathfrak{S}_{pj}x(t)\,|\,\mathfrak{k}_{\mathfrak{h}}x(t) = \pm\beta_{\mathfrak{h}}\right\} \geq 1 + \theta\gamma^2. \quad (39)
$$

Define the Lagrange function $L(x(t)) = x^T(t)\mathfrak{S}_{pj}x(t) + \varepsilon(\mathfrak{k}_{\mathfrak{h}}x(t) \mp \beta_{\mathfrak{h}})$ with Lagrange factor ε, it has

$$
\begin{cases}
\dfrac{\partial L(x(t))}{\partial x(t)} = 2x^T(t)\mathfrak{S}_{pj} + \varepsilon\mathfrak{k}_{\mathfrak{h}} = 0, \\
\mathfrak{k}_{\mathfrak{h}}x(t) \mp \beta_{\mathfrak{h}} = 0.
\end{cases} \quad (40)
$$

Solving (40), we obtain $\varepsilon^* = \mp 2\beta_{\mathfrak{h}}(\mathfrak{k}_{\mathfrak{h}}\mathfrak{S}^{-1}_{pj}\mathfrak{k}^T_{\mathfrak{h}})^{-1}$, $x^*(t) = \pm\beta_{\mathfrak{h}}\mathfrak{S}^{-1}_{pj}\mathfrak{k}^T_{\mathfrak{h}}(\mathfrak{k}_{\mathfrak{h}}\mathfrak{S}^{-1}_{pj}\mathfrak{k}^T_{\mathfrak{h}})^{-1}$. Substituting $x^*(t)$ into (39) and applying Schur complement, we have

$$
\begin{bmatrix} \frac{\beta^2_{\mathfrak{h}}}{1+\theta\gamma^2} & \mathfrak{k}_{\mathfrak{h}} \\ * & \mathfrak{S}_{pj} \end{bmatrix} \geq 0. \quad (41)
$$

Theorem 2: Giving constants $\kappa \geq 1$, $d \geq 0$, $\delta > 0$, $\gamma > 0$, $\theta > 0$, and $\beta_{\mathfrak{h}} > 0$, the trajectories of system (16) starting from $\bar{\mathcal{D}}_1$ will stay in $\bar{\mathcal{D}}_2$ for time $t > d$, if there exist positive definite matrices $\tilde{Q}_{pj}$, $\tilde{S}_{bj} \in R^{2n\times 2n}$, $\tilde{R}_{1pj}$, $\tilde{R}_{cj}$, $\tilde{\Omega}_p$, $\mathfrak{S}^*_{pj} \in R^{n\times n}$, matrices $\tilde{U}_{gj}$, $G \in R^{n\times n}$, $\mathcal{Z}_{\vartheta j} \in R^{l\times n}$, such that (19) and the following inequalities hold for $p \in \mathcal{N}$, $\vartheta \in \mathcal{O}$, $\mathcal{K} \in \left\{\kappa, \frac{1}{\kappa}\right\}$, $b = 1,2$, $c = 1,2,3$, $f = 1,2,4$, $g = 1,2,3,4$, $\mathfrak{h} = 1,2,\ldots,n$

$$
\begin{bmatrix} \tilde{\Theta}^2_{p\vartheta ii} & \tilde{\Theta}^{4T}_{p\vartheta ii} \\ * & -I \end{bmatrix} < 0, \quad (42)
$$

$$
\begin{bmatrix} \tilde{\Theta}^2_{p\vartheta ij} + \mathcal{K}\tilde{\Theta}^2_{p\vartheta ji} & \tilde{\Theta}^{4T}_{p\vartheta ij} & \sqrt{\kappa}\tilde{\Theta}^{4T}_{p\vartheta ji} \\ * & -I & 0 \\ * & * & -I \end{bmatrix} < 0, \quad (43)
$$

$$
\sum_{q=1}^{N}\pi_{pq}\tilde{R}_{1qj} - \tilde{R}_{1j} \leq 0, \quad (44)
$$

$$
\tilde{\Psi}_j \geq 0, \quad (45)
$$

$$
\begin{bmatrix} \Xi_{pj} & \frac{\sqrt{2}}{2}G \\ * & -I \end{bmatrix} \leq 0, \quad (46)
$$

$$
\begin{bmatrix} \frac{\beta^2_{\mathfrak{h}}}{1+\theta\gamma^2} & \mathfrak{k}_{\mathfrak{h}}G^T \\ * & \mathfrak{S}^*_{pj} \end{bmatrix} \geq 0, \quad (47)
$$

where

$$
\begin{aligned}
\tilde{\Psi}_j &= \begin{bmatrix} \hat{R}_{2j} & \tilde{U}_j \\ * & \hat{R}_{2j} \end{bmatrix}, \tilde{U}_j = \begin{bmatrix} \tilde{U}_{1j} & \tilde{U}_{2j} \\ \tilde{U}_{3j} & \tilde{U}_{4j} \end{bmatrix}, \\
\tilde{\Theta}^2_{p\vartheta ij} &= \tilde{\Theta}^1_{p\vartheta ij} - \gamma^2 e^T_{10}e_{10}, \\
\tilde{\Theta}^1_{p\vartheta ij} &= \tilde{\Theta}^*_{p\vartheta ij} + e^T_4\tilde{\Omega}_p e_4 + e^T_9(\tilde{\Omega}_p - \delta\tilde{\Omega}_p)e_9 + 2e^T_4\tilde{\Omega}_p e_9, \\
\tilde{\Theta}^*_{p\vartheta ij} &= sym(\Gamma^T_1\tilde{Q}_{pj}\Gamma_2 + \tilde{\mathcal{F}}^T_0\tilde{\Im}_{p\vartheta ij}) + \Gamma^T_1\sum_{q=1}^{N}\pi_{pq}\tilde{Q}_{qj}\Gamma_1 \\
&\quad + e^T_1(\tilde{R}_{1pj} + d\tilde{R}_{1j})e_1 - e^T_3\tilde{R}_{1pj}e_3 + e^T_2(d^2\tilde{R}_{2j} \\
&\quad + \frac{1}{2}d^2\tilde{R}_{3j})e_2 - \Gamma^T_5\tilde{S}_{1j}\Gamma_5 + 2\Gamma^T_5\tilde{S}_{1j}\Gamma_6 + \Gamma^T_7\tilde{S}_{2j}\Gamma_7 \\
&\quad + 2\Gamma^T_7\tilde{S}_{2j}\Gamma_8 - \Gamma^T_3\tilde{\Psi}_j\Gamma_3 - \Gamma^T_4\hat{R}_{3j}\Gamma_4, \\
\tilde{\Theta}^4_{p\vartheta ij} &= col\left\{\sqrt{\sigma_{p1}}\tilde{\mathcal{Y}}_{p1ij}, \sqrt{\sigma_{p2}}\tilde{\mathcal{Y}}_{p2ij}, \ldots, \sqrt{\sigma_{pO}}\tilde{\mathcal{Y}}_{pOij}\right\}, \\
\tilde{\mathcal{F}}_0 &= e_1 + e_2, \tilde{\Im}_{p\vartheta ij} = -G^Te_2 + A_{pi}G^Te_1 \\
&\quad + \sum_{\vartheta=1}^{O}\sigma_{p\vartheta}B_{1pi}\mathcal{Z}_{\vartheta j}(e_4 + e_9) + D_{pi}e_{10}, \\
\tilde{\mathcal{Y}}_{p\vartheta ij} &= C_{pi}G^Te_1 + B_{2pi}\mathcal{Z}_{\vartheta j}(e_4 + e_9) + E_{pi}e_{10}, \\
\Xi_{pj} &= \frac{1}{2}d^3\tilde{R}_{2j} + \frac{1}{6}d^3\tilde{R}_{3j} + d\tilde{R}_{1pj} + \frac{1}{2}d^2\tilde{R}_{1j} + \tilde{Q}_{1pj} \\
&\quad + \tilde{Q}_{2pj} + d^2(\tilde{Q}_{2pj} + \tilde{Q}_{4pj}) + d\sum_{b=1}^{2}(\tilde{S}^1_{bj} \\
&\quad + 2\tilde{S}^2_{bj} + \tilde{S}^4_{bj}) - \mathfrak{S}^*_{pj}, \\
\hat{R}_{2j} &= diag\left\{\tilde{R}_{2j}, 3\tilde{R}_{2j}\right\}, \hat{R}_{3j} = diag\left\{2\tilde{R}_{3j}, \tilde{4}R_{3j}\right\}, \\
\bar{G} &= diag\{G, G\}, \mathfrak{S}^*_{pj} = G\mathfrak{S}_{pj}G^T, \\
\tilde{Q}_{pj} &= \bar{G}Q_{pj}\bar{G}^T, \tilde{S}_{bj} = \bar{G}S_{bj}\bar{G}^T, \tilde{R}_{1pj} = GR_{1pj}G^T,
\end{aligned}
$$

$\tilde{R}_{cj}=GR_{cj}G^T, \tilde{U}_{gj}=GU_{gj}G^T, \tilde{Q}_{fpj}=GQ_{fpj}G^T,$
$\tilde{S}^f_{bj}=GS^f_{bj}G^T, \tilde{\Omega}_p=G\Omega_pG^T,$

and the controller gain is

$$K_{\vartheta j}=\mathcal{Z}_{\vartheta j}G^{-T}. \tag{48}$$

*Proof:*Define

$$\mathcal{G}_1=diag\left\{\bar{\mathcal{G}},\bar{\mathcal{G}},G,I,\bar{\mathcal{I}}\right\}, \mathcal{G}_2=diag\left\{\bar{\mathcal{G}},\bar{\mathcal{G}},G,I,\bar{\mathcal{I}},\bar{\mathcal{I}}\right\},$$
$$\bar{\mathcal{G}}=diag\left\{G,G,G,G\right\}, \bar{\mathcal{I}}=diag\overbrace{\left\{I,I,...,I\right\}}^{O},$$
$$\hat{\mathcal{G}}=diag\left\{I,G\right\}, G=F^{-1},$$

based on Schur complement, pre- and post- multiply (22)-(25), (36), (41) by $\mathcal{G}_1$, $\mathcal{G}_2$, G, $\bar{\mathcal{G}}$, G, $\hat{\mathcal{G}}$ and the transpositions, we have (42)-(47). ■

The number of decision variables in Theorem 2 can be calculated as $rn(3.5+9.5n+2p+3np+l\vartheta)+0.5pn^2+0.5np+n^2$. Hence, the computational complexity is contingent upon the values of modes p, ϑ, orders n, l, and rules r.

According to Remark 1, the controller design approach based on TETM (6) is presented in the corollary as follows.

Corollary 1: Giving constants $\kappa\geq 1$, $d\geq 0$, $0\leq\delta^*<1$, $\gamma>0$, $\theta>0$, and $\beta_{\mathfrak{h}}>0$, the trajectories of system (16) starting from $\bar{\mathcal{D}}_1$ will stay in $\bar{\mathcal{D}}_2$ for time $t>d$, if there exist positive definite matrices $\tilde{Q}_{pj}$, $\tilde{S}_{bj}\in R^{2n\times 2n}$, $\tilde{R}_{1pj}$, $\tilde{R}_{cj}$, $\tilde{\Omega}_p$, $\mathfrak{S}^*_{pj}\in R^{n\times n}$, matrices $\tilde{U}_{gj}$, $G\in R^{n\times n}$, $\mathcal{Z}_{\vartheta j}\in R^{l\times n}$, such that (19), (44)-(47) and the following inequalities hold for $p\in\mathcal{N}$, $\vartheta\in\mathcal{O}$, $\mathcal{K}\in\left\{\kappa,\frac{1}{\kappa}\right\}$, $b=1,2$, $c=1,2,3$, $f=1,2,4$, $g=1,2,3,4$, $\mathfrak{h}=1,2,\ldots,n$

$$\begin{bmatrix} \hat{\Theta}^2_{p\vartheta ii} & \tilde{\Theta}^{4T}_{p\vartheta ii} \\ * & -I \end{bmatrix}<0, \tag{49}$$

$$\begin{bmatrix} \hat{\Theta}^2_{p\vartheta ij}+\mathcal{K}\hat{\Theta}^2_{p\vartheta ji} & \tilde{\Theta}^{4T}_{p\vartheta ij} & \sqrt{\kappa}\tilde{\Theta}^{4T}_{p\vartheta ji} \\ * & -I & 0 \\ * & * & -I \end{bmatrix}<0, \tag{50}$$

where

$\hat{\Theta}^2_{p\vartheta ij}=\hat{\Theta}^1_{p\vartheta ij}-\gamma^2e^T_{10}e_{10},$
$\hat{\Theta}^1_{p\vartheta ij}=\tilde{\Theta}^*_{p\vartheta ij}+e^T_4\delta^*\tilde{\Omega}_pe_4+e^T_9(\delta^*\tilde{\Omega}_p-\tilde{\Omega}_p)e_9+2e^T_4\delta^*\tilde{\Omega}_pe_9.$

Proof: The process is the same as Theorem 2, thus being omitted.

IV. Illustrative Examples

Example 1: To prove the practicability of our method, a mass-spring-damper mechanical system is considered as follows [2], [4], [38]:

$$M\ddot{\mathfrak{s}}(t)+D\dot{\mathfrak{s}}(t)+f(\mathfrak{s}(t))=\phi(\dot{\mathfrak{s}}(t))u(t)+w(t),$$

where M is the mass, D denotes the viscous damping, $u(t)$ is the force, $w(t)$ is the disturbance, and $\mathfrak{s}(t)$ is the position. $\phi(\dot{\mathfrak{s}}(t))$ and $f(\mathfrak{s}(t))$ are associated with the input and spring. Assume that $x(t)=\begin{bmatrix}\dot{\mathfrak{s}}^T(t) & \mathfrak{s}^T(t)\end{bmatrix}^T$, $\phi(\dot{\mathfrak{s}}(t))=1+g_1\dot{\mathfrak{s}}^3(t)$, $f(\mathfrak{s}(t))=g\mathfrak{s}(t)$ $(g\in[g_2,g_3])$, $\mathfrak{s}(t)\in[-1.5,1.5]$, $\dot{\mathfrak{s}}(t)\in[-1.5,1.5]$, $M=1$, $D=1$, $g_1=0.13$, $g_2=0.5$, $g_3=1.81$.

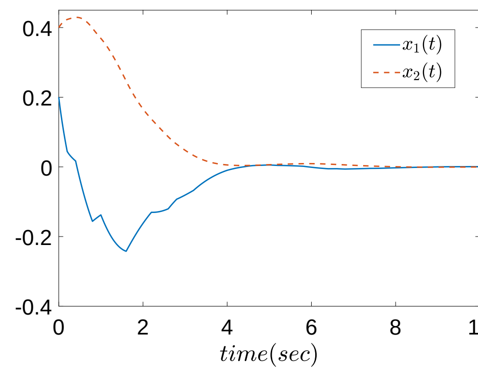

Fig. 2. The state responses (Example 1).

Considering the stochastic variations observed in system parameters and structure, we assume two jump modes, accompanied by the following TP matrix:

$$\Pi_1=\begin{bmatrix} -3 & 3 \\ 4 & -4 \end{bmatrix}.$$

Applying the method in [2] and [38], with $h_1=0.5+\frac{x_1^3(t)}{6.75}$, $h_2=0.5-\frac{x_1^3(t)}{6.75}$, the nonlinear system can be represented by the FMJSs with the following parameters:

$$A_{11}=\begin{bmatrix} -1 & -1.155 \\ 1 & 0 \end{bmatrix}, A_{21}=\begin{bmatrix} -1 & -2.210 \\ 1 & 0 \end{bmatrix},$$
$$A_{12}=\begin{bmatrix} -1 & -1.155 \\ 1 & 0 \end{bmatrix}, A_{22}=\begin{bmatrix} -1 & -2.210 \\ 1 & 0 \end{bmatrix},$$
$$B_{111}=\begin{bmatrix} 1.4387 \\ 0 \end{bmatrix}, B_{121}=\begin{bmatrix} 0.5755 \\ 0 \end{bmatrix},$$
$$B_{112}=\begin{bmatrix} 0.5613 \\ 0 \end{bmatrix}, B_{122}=\begin{bmatrix} 0.2245 \\ 0 \end{bmatrix},$$
$$B_{211}=B_{212}=\begin{bmatrix} 0 \\ 1 \end{bmatrix}, B_{221}=B_{222}=\begin{bmatrix} 0 \\ 0.8 \end{bmatrix},$$
$$D_{\theta(t)1}=D_{\theta(t)2}=\begin{bmatrix} 1 \\ 0 \end{bmatrix}, C_{\theta(t)1}=C_{\theta(t)2}=\begin{bmatrix} 0 & 1 \\ 0 & 0 \end{bmatrix}.$$

Furthermore, the constraints related to MFs are as follows: if $\dot{h}_1<0$, we have

$$\mathfrak{G}_{1(p=1,2)}=\left\{\begin{array}{l} Q_{p1}-Q_{p2}>0, R_{1p1}-R_{1p2}>0, \\ R_{c1}-R_{c2}>0, S_{b1}-S_{b2}>0, \end{array}\right\},$$

if $\dot{h}_1\geq 0$, we have

$$\mathfrak{G}_{2(p=1,2)}=\left\{\begin{array}{l} Q_{p1}-Q_{p2}\leq 0, R_{1p1}-R_{1p2}\leq 0, \\ R_{c1}-R_{c2}\leq 0, S_{b1}-S_{b2}\leq 0, \end{array}\right\},$$

with $c=1,2,3$, $b=1,2$.

Letting $d=0.8$, $\kappa=1.1$, $\delta=30$, $\theta=1/4$, $\mathcal{T}=0.08$, $\mathfrak{k}_1=\begin{bmatrix}1 & 0\end{bmatrix}$, $\mathfrak{k}_2=\begin{bmatrix}0 & 1\end{bmatrix}$, $\mathbb{C}=\{x(t):|x_{\mathfrak{h}}(t)|\leq 1.5, \mathfrak{h}=1,2\}$, Table II illustrates the optimal H_∞ index γ obtained by different approaches. For example, in case III, the optimal H_∞ index γ is $\gamma_1=0.5548$ under $\mathfrak{G}_{1(p=1,2)}$ and $\gamma_2=0.5548$ under $\mathfrak{G}_{2(p=1,2)}$. Hence, the final optimal H_∞ index γ is determined as $\gamma_{\min}=\min\{\gamma_1,\gamma_2\}=0.5548$, indicating that the approach presented in this article

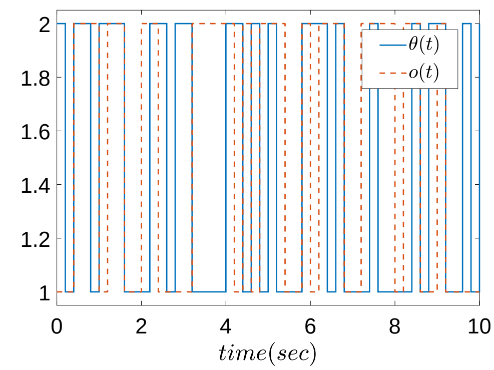

Fig. 3. The trajectories of $\theta(t)$ and $o(t)$ (Example 1).

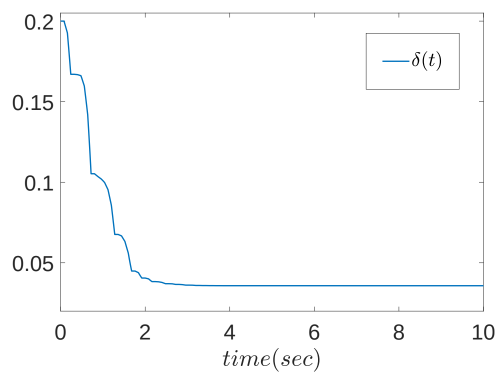

Fig. 4. Variation of $\delta(t)$ (Example 1).

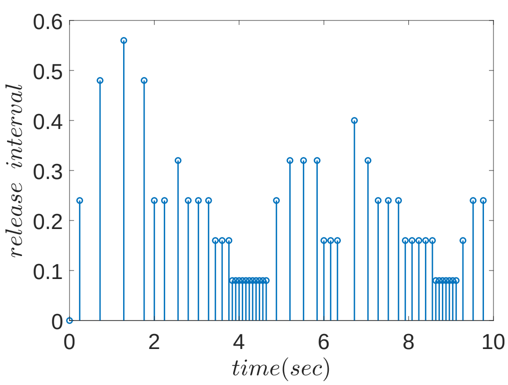

Fig. 5. AETM triggering instants (Example 1).

is less conservative than [38]. Meanwhile, when applying identical parameters, the value of γ obtained through the switching method in [7], [8] is 0.5627, which means that the method proposed in this paper offers a more comprehensive theoretical framework with a relatively modest impact on H_∞ performance. Moreover, Table I presents the CP matrices including synchronous case, partially asynchronous case, and completely asynchronous case. From Table II, we can find that the optimal H_∞ index γ becomes bigger as asynchrony intensifies.

Especially, in case III, take $\gamma = 1.8$, the corresponding

TABLE I
CONDITIONAL PROBABILITY Π_2 (EXAMPLE 1)

	case I	case II	case III
Π_2	$\begin{bmatrix} 1 & 0 \\ 0 & 1 \end{bmatrix}$	$\begin{bmatrix} 1 & 0 \\ 0.4 & 0.6 \end{bmatrix}$	$\begin{bmatrix} 0.2 & 0.8 \\ 0.4 & 0.6 \end{bmatrix}$

TABLE II
OPTIMAL γ FOR DIFFERENT CONDITIONAL PROBABILITIES (EXAMPLE 1)

$\gamma_{\min}$	case I	case II	case III
Theorem 2	0.5536	0.5539	0.5548
[38]	0.9046	0.9074	0.9159

TABLE III
DATA TRANSMISSION RATE FOR DIFFERENT $\delta(0)$ (EXAMPLE 1)

$\delta(0)$	0.1	0.2	0.4	0.6	0.8
Triggering times	57	52	37	25	19
Transmission rate	45.6%	41.6%	29.6%	20.0%	15.2%

controller matrices are

$$\begin{aligned}
K_{11}^1 &= \begin{bmatrix} -0.12 & -0.03 \end{bmatrix}, K_{12}^1 = \begin{bmatrix} -0.07 & -0.02 \end{bmatrix}, \\
K_{21}^1 &= \begin{bmatrix} -0.13 & -0.14 \end{bmatrix}, K_{22}^1 = \begin{bmatrix} -0.09 & -0.08 \end{bmatrix}, \\
K_{11}^2 &= \begin{bmatrix} -0.04 & 0.00 \end{bmatrix}, K_{12}^2 = \begin{bmatrix} -0.12 & -0.04 \end{bmatrix}, \\
K_{21}^2 &= \begin{bmatrix} -0.05 & -0.04 \end{bmatrix}, K_{22}^2 = \begin{bmatrix} -0.14 & -0.11 \end{bmatrix}.
\end{aligned}$$

Under the initial conditions $x(0) = \begin{bmatrix} 0.2 & 0.4 \end{bmatrix}^T$, the disturbance $w(t) = \sqrt{t}e^{-t}$ with bounded energy ($\int_0^t w^T(t)w(t)dt \leq \theta = 1/4$), the triggering times and data transmission rate for different $\delta(0)$ are illustrated in Table III. It can be seen that the triggering times and data transmission rate decrease as $\delta(0)$ increases. In particular, with $\delta(0) = 0.2$, Figure 2 and Figure 3 illustrate the state responses and asynchronous Markov stochastic processes, demonstrating the effectiveness of the proposed asynchronous controller design approach. Figure 4 plots the trajectory of adaptive triggering parameter $\delta(t)$, which is dynamically adjusted and eventually approaches 0.0345. Based on AETM, the release instants are shown in Figure 5. Furthermore, Figure 6 depicts the trajectories of dh_1/dt and control input u, with switching points $L_1\,(t = 0.8)$, $L_2\,(t = 1)$, $L_3\,(t = 1.6)$, and $\dot{h}_1(0.8) = 0.0011$, $\dot{h}_1(1) = -0.0026$, $\dot{h}_1(1.6) = 0.0058$. It can be observed that the controller exhibits a pronounced switching behavior, where it is u_1 within the time interval $[0, L_1]$, switches to u_2 during the time interval $[L_1, L_2]$, reverts back to u_1 within the time interval $[L_2, L_3]$, and ultimately switches to u_2 in the time interval $[L_3, +\infty]$. Besides, Figure 7 shows the sets $\bar{\mathcal{D}}_1$, $\bar{\mathcal{D}}_2$, and the responses of four initial states from the boundary. We can observe that two trajectories leave $\bar{\mathcal{D}}_1$ but stay in $\bar{\mathcal{D}}_2$ and return to $\bar{\mathcal{D}}_1$ soon, which confirms our conclusion.

Example 2: When $\mathcal{N} = \{1\}$, consider the two-rule fuzzy system with the following parameters [20], [22]:

$$A_1 = \begin{bmatrix} -2 & 0 \\ 0 & -0.9 \end{bmatrix}, A_2 = \begin{bmatrix} -1 & 0.5 \\ 0 & -1 \end{bmatrix},$$

$$B_{11} = \begin{bmatrix} -1 & 0 \\ -1 & -1 \end{bmatrix}, B_{12} = \begin{bmatrix} -1 & 0 \\ 0.1 & -1 \end{bmatrix},$$

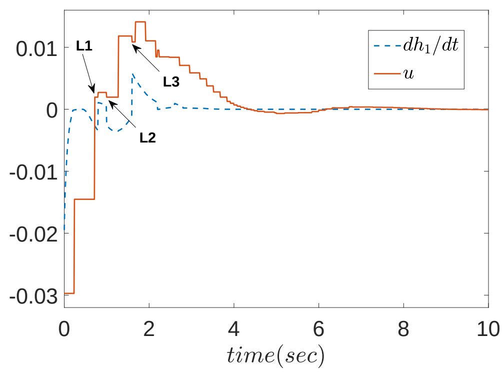

Fig. 6. The trajectories of dh_1/dt and control input u (Example 1).

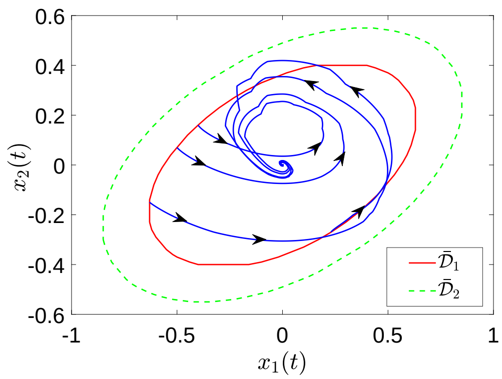

Fig. 7. The sets $\bar{\mathcal{D}}_1$, $\bar{\mathcal{D}}_2$ and four trajectories starting on the boundary of $\bar{\mathcal{D}}_1$ (Example 1).

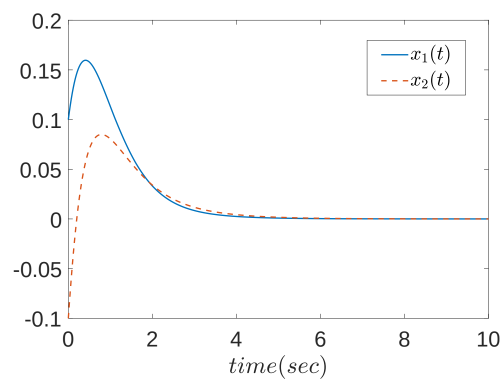

Fig. 8. The state responses (Example 2).

$$B_{21} = \begin{bmatrix} 0.4 & 0.2 \\ 0.1 & 0.7 \end{bmatrix}, B_{22} = \begin{bmatrix} 0.3 & 0.5 \\ 0.2 & 0.6 \end{bmatrix},$$
$$D_1 = \begin{bmatrix} 0.5 & 0.4 \\ 0.2 & 0.3 \end{bmatrix}, D_2 = \begin{bmatrix} 0.1 & 0.6 \\ 0.8 & 0.7 \end{bmatrix},$$
$$C_1 = \begin{bmatrix} 0.1 & 0.3 \\ 0.4 & 0.6 \end{bmatrix}, C_2 = \begin{bmatrix} 0.5 & 0.1 \\ 0.4 & 0.1 \end{bmatrix},$$
$$h_1 = \frac{1 - \sin(x_1(t))}{2}, h_2 = 1 - h_1.$$

Setting $\mathbb{C} = \left\{x(t) : |x_{\mathfrak{h}}(t)| \le \frac{\pi}{2}, \mathfrak{h} = 1, 2\right\}$, $d = 0.5$, $\kappa =$ 1.5, $\theta = 1/3$, Table IV lists the minimum H_∞ performance index γ for different values of δ^*. We can observe that under the same δ^*, the minimum H_∞ performance γ obtained by Corollary 1 is smaller than that obtained by [20], [22], [27].

TABLE IV
THE MINIMUM VALUE OF γ FOR DIFFERENT δ^* (EXAMPLE 2)

$\gamma_{\min}$	$\delta^* = 0$	$\delta^* = 0.10$	$\delta^* = 0.15$	$\delta^* = 0.25$
[27]	1.2499	2.3560	2.8715	4.2290
[20]	1.0078	1.4009	1.5462	1.8615
[22]	0.5627	0.6503	0.6700	0.7005
Corollary 1	0.3836	0.3895	0.3904	0.3913

TABLE V
THE MAXIMUM VALUE OF d FOR DIFFERENT δ^* (EXAMPLE 2)

$d_{\max}$	$\delta^* = 0$	$\delta^* = 0.10$	$\delta^* = 0.15$	$\delta^* = 0.25$
[20]	0.8755	0.6014	0.5583	0.4978
Corollary 1	1.4636	1.4175	1.4120	1.4067

TABLE VI
THE MINIMUM VALUE OF γ FOR DIFFERENT δ^* AND κ (EXAMPLE 2)

$\gamma_{\min}$	Methods	$\delta^* = 0$	$\delta^* = 0.10$	$\delta^* = 0.15$	$\delta^* = 0.25$
$\kappa = 1.0$	[20]	0.8984	0.9543	0.9832	1.0453
	Corollary 1	0.2425	0.2540	0.2557	0.2579
$\kappa = 2.5$	[20]	1.0181	1.2511	1.3201	1.4469
	Corollary 1	0.2699	0.2838	0.2868	0.2909

For simulation, assume $\delta = 2$, $\gamma = 1.5$, $\mathcal{T} = 0.1$, initial conditions $x(0) = \begin{bmatrix} 0.1 & -0.1 \end{bmatrix}^T$, energy-bounded disturbance $w(t) = \begin{bmatrix} e^{-6t}\sin(t) & e^{-2t}\cos(t) \end{bmatrix}^T$, the state responses is described in Figure 8. Figure 9 illustrates the trajectories of dh_1/dt and control input u, with switching points $J\,(t = 0.42)$, and $\dot{h}_1(0.42) = 0.0024$. Observably, the controller is u_1 in the interval $[0, J]$ and then switches to u_2 in the interval $[J, +\infty]$. Meanwhile, the trajectory of $\delta(t)$ is shown in Figure 10, which is dynamically adjusted and finally tends to 0.1356. Based on AETM, the release instants are shown in Figure 11, and the data transmission rate is 23%. On the premise that other parameters remain unchanged, define $\delta^* = 0.05$, the TETM (6) is considered. The corresponding release instants are given in Figure 12, and the data transmission rate is 38%. Compared with Figure 11, it can be deduced that the AETM presented in this paper can save more communication resources than TETM.

Letting $\gamma = 0.7$, $\kappa = 1$, under the same parameters as [20], the maximum value of d for different values of δ^* are presented in Table V. For example, when $\delta^* = 0$, the maximum value of d is $d_1 = 2.1109$ under the constraint $\mathfrak{G}_1$ and $d_2 = 1.4636$ under the constraint $\mathfrak{G}_2$. Hence, the final maximum value of d obtained by Corollary 1 is $d_{\max} = \min\{d_1, d_2\} = 1.4636$, which is larger than that obtained by [20].

Similar to [20], the relationship between γ, κ and δ^* is analyzed with $d = 0.3$, and the corresponding results are listed in Table VI. From Table VI, it is evident that the index γ increases as δ^* or κ increases, which indirectly indicates the importance of considering asynchronous premise variables. Furthermore, under the same δ^* and κ, Corollary 1 yields smaller results compared to [20], implying that the method

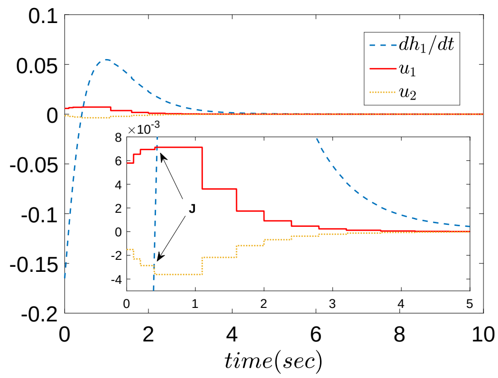

Fig. 9. The trajectories of dh_1/dt and control input u (Example 2).

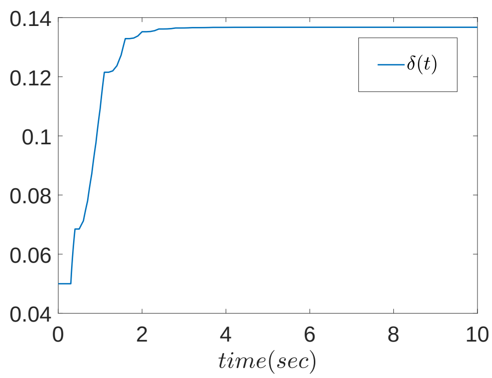

Fig. 10. Variation of $\delta(t)$ (Example 2).

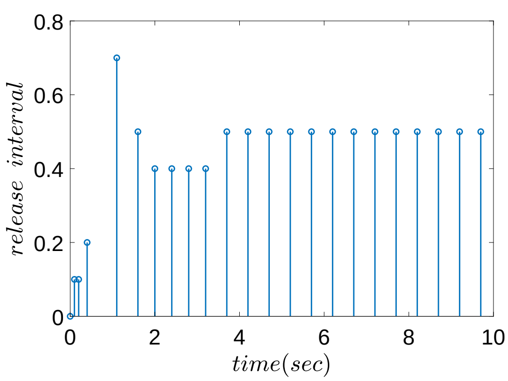

Fig. 11. AETM triggering instants (Example 2).

presented in this article is less conservative than [20].

V. Conclusion

This article has considered the double asynchronous switching H_∞ control problem for FMJSs based on AETM. A MFs-dependent LKF has been constructed, and the DPT terms have been introduced to further reduce conservatism. Furthermore, a novel double asynchronous switching controller has been presented, employing the time derivative of MFs, and a switching AETM has been proposed to avoid the unnecessary transmission. Ultimately, the validity of the presented work

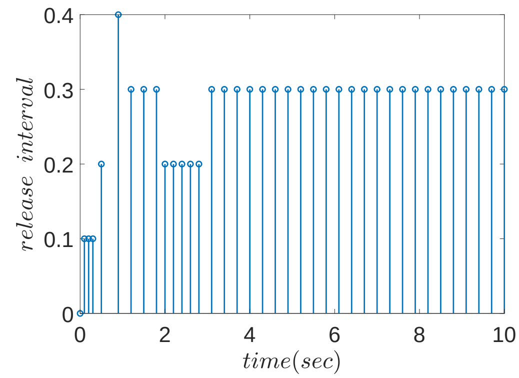

Fig. 12. TETM triggering instants (Example 2).

has been demonstrated by two numerical examples. Notably, the conservative reduction in this paper comes at the expense of increased computational complexity, and the dynamic characteristics of FMJSs may change over time and with variations in external conditions. Hence, it is essential to extend our approach to adaptive control and explore a technique that can further reduce computational complexity.

References

[1] T. Takagi and M. Sugeno, Fuzzy identification of systems and its applications to modeling and control. IEEE Transactions on Systems, Man, and Cybernetics: Systems 15 (1985) 116-132.

[2] K. Tanaka, T. Ikeda, and H. O. Wang, Robust stabilization of a class of uncertain nonlinear systems via fuzzy control: Quadratic stabilizability, H_∞ control theory, and linear matrix inequalities. IEEE Transactions on Fuzzy Systems 4 (1996) 1-13.

[3] X. P. Guan and C. L. Chen, Delay-dependent guaranteed cost control for T-S Fuzzy systems with time delays. IEEE Transactions on Fuzzy Systems 12 (2004) 236-249.

[4] H. N. Wu, Reliable robust H_∞ fuzzy control for uncertain nonlinear systems with Markovian jumping actuator faults. Journal of Dynamic Systems, Measurement, and Control 129 (2007) 252-261.

[5] H. Y. Li, J. Y. Yu, C. Hilton, and H. H. Liu, Adaptive sliding-mode control for nonlinear active suspension vehicle systems using T-S fuzzy approach. IEEE Transactions on Industrial Electronics 60 (2013) 3328-3338.

[6] Y. F. Mu, H. G. Zhang, Z. Y. Gao, and J. Zhang, A fuzzy Lyapunov function approach for fault estimation of T-S Fuzzy fractional-order systems based on unknown input observer. IEEE Transactions on Systems, Man, and Cybernetics: Systems 53 (2023) 1246-1255.

[7] L. Wang and H.-K. Lam, A New approach to stability and stabilization analysis for continuous-time Takagi-Sugeno fuzzy systems with time delay. IEEE Transactions on Fuzzy Systems 26 (2018) 2460-2465.

[8] L. Wang and H.-K. Lam, H_∞ control for continuous-time Takagi-Sugeno fuzzy model by applying generalized Lyapunov function and introducing outer variables. Automatica 125 (2021) 109409.

[9] Y. B. Wang, C. C. Hua, and P. G. Park, A generalized reciprocally convex inequality on stability and stabilization for T-S fuzzy systems with time-varying delay. IEEE Transactions on Fuzzy Systems 31 (2023) 722-733.

[10] H. Y. Li, Y. Y. Wang, D. Y. Yao, and R. Q. Lu, A sliding mode approach to stabilization of nonlinear Markovian jump singularly perturbed systems. Automatica 97 (2018) 404-413.

[11] Y. F. Tian and Z. S. Wang, Extended dissipativity analysis for Markovian jump neural networks via double-integral-based delay-product-type Lyapunov functional. IEEE Transactions on Neural Networks and Learning Systems 32 (2021) 3240-3246.

[12] Y. Pan, W. Ji, H. K. Lam, and L. Cao, An improved predefined-time adaptive neural control approach for nonlinear multiagent systems. IEEE Transactions on Automation Science and Engineering. Doi:10.1109/TASE.2023.3324397.

[13] S. L. Dong, C. L. P. Chen, M. Fang, and Z.-G. Wu, Dissipativity-based asynchronous fuzzy sliding mode control for T-S fuzzy hidden Markov jump systems. IEEE Transactions on Cybernetics 50 (2020) 4020-4030.
[14] C. C. Ren, S. P. He, X. L. Luan, F. Liu, and H. R. Karimi, Finite-time L_2-gain asynchronous control for continuous-time positive hidden Markov jump systems via T-S fuzzy model approach. IEEE Transactions on Cybernetics 51 (2021) 77-87.
[15] L. X. Zhu, Y. Q. Wang, G. M. Zhuang, and G. F. Song, Dynamic-memory event-based asynchronous security control for T-S fuzzy singular semi-Markov jump systems against multi-cyber attacks. Journal of the Franklin Institute 360 (2023) 424-457.
[16] S. B. Ding, Z. S. Wang, and N. N. Rong, Intermittent control for quasisynchronization of delayed discrete-time neural networks. IEEE Transactions on Cybernetics 51 (2021) 862-873.
[17] S. B. Ding, Z. S. Wang, and X. P. Xie, Periodic event-triggered synchronization for discrete-time complex dynamical networks. IEEE Transactions on Neural Networks and Learning Systems 33 (2022) 3622-3633.
[18] J. Guo, R. Z. Jia, R. N. Su, and Y. L. Zhao, Identification of FIR systems with binary-valued observations against data tampering attacks. IEEE Transactions on Systems, Man, and Cybernetics: Systems 53 (2023) 5861-5873.
[19] H. R. Ren, Z. J. Cheng, J. H. Qin, and R. Q. Lu, Deception attacks on event-triggered distributed consensus estimation for nonlinear systems. Automatica 154 (2023) 111100.
[20] H. Shen, F. Li, H. C. Yan, H. R. Karimi, and H.-K. Lam, Finite-time event-triggered H_∞ control for T-S fuzzy Markov jump systems. IEEE Transactions on Fuzzy Systems 26 (2018) 3122-3135.
[21] J. Guo and J. D. Diao, Prediction-based event-triggered identification of quantized input FIR systems with quantized output observations. Science China Information Sciences 63 (2020) 112201.
[22] W. Q. Xie, S. K. Nguang, H. Zhu, Y. P. Zhang, and K. B. Shi, A novel event-triggered asynchronous H_∞ control for T-S fuzzy Markov jump systems under hidden Markov switching topologies. Fuzzy Sets and Systems 443 (2022) 258-282.
[23] W. X. Zhou, J. Fu, H. C. Yan, X. Du, Y. Y. Wang, and H. Zhou, Event-triggered approximate optimal path-following control for unmanned surface vehicles with state constraints. IEEE Transactions on Neural Networks and Learning Systems 34 (2023) 104-118.
[24] G. T. Ran, C. J. Li, R. Sakthivel, C. S. Han, B. H. Wang, and J. Liu, Adaptive event-triggered asynchronous control for interval type-2 fuzzy Markov jump systems with cyberattacks. IEEE Transactions on Control of Network Systems 9 (2022) 88-99.
[25] J. Liu, G. T. Ran, Y. Q. Huang, C. S. Han, Y. Yu, and C. Y. Sun, Adaptive event-triggered finite-time dissipative filtering for interval type-2 fuzzy Markov jump systems with asynchronous modes. IEEE Transactions on Cybernetics 52 (2022) 9709-9721.
[26] Y. W. Qi, S. Yuan, and B. Niu, Asynchronous control for switched T-S fuzzy systems subject to data injection attacks via adaptive event-triggering schemes. IEEE Transactions on Systems, Man, and Cybernetics: Systems 52 (2022) 4658-4670.
[27] C. Peng, D. Yue, and Q.-L. Han, Communication and control for networked complex systems. Berlin, Germany: Springer-Verlag, 2015.
[28] J. Zhang and C. Peng, Event-triggered H_∞ filtering for networked Takagi-Sugeno fuzzy systems with asynchronous constraints. IET Signal Processing 9 (2015) 403-411.
[29] H. Y. Li, Z. X. Zhang, H. C. Yan, and X. P. Xie, Adaptive event-triggered fuzzy control for uncertain active suspension systems. IEEE Transactions on Cybernetics 49 (2019) 4388-4397.
[30] M. Xue, H. C. Yan, H. Zhang, J. Sun, and H.-K. Lam, Hidden-Markov-model-based asynchronous H_∞ tracking control of fuzzy Markov jump systems. IEEE Transactions on Fuzzy Systems 29 (2021) 1081-1092.
[31] S. Wang and Z.-G. Wu, Asynchronous control of uncertain Markov jump systems with actuator saturation. IEEE Transactions on Circuits and Systems II: Express Briefs 69 (2022) 3269-3273.
[32] X. H. Li, C. K. Ahn, W. D. Zhang, and P. Shi, Asynchronous event-triggered-based control for stochastic networked Markovian jump systems with FDI attacks. IEEE Transactions on Systems, Man, and Cybernetics: Systems 53 (2023) 5955-5967.
[33] Y. F. Zhang and Z.-G. Wu, Asynchronous control of Markov jump systems under aperiodic DoS attacks. IEEE Transactions on Circuits and Systems II: Express Briefs 70 (2023) 685-689.
[34] Y. L. Wei, J. B. Qiu, P. Shi, and H.-K. Lam, A new design of H-infinity piecewise filtering for discrete-time nonlinear time-varying delay systems via T-S fuzzy affine models. IEEE Transactions on Systems, Man, and Cybernetics: Systems 47 (2017) 2034-2047.
[35] X. Z. Yang, H.-K. Lam, and L. G. Wu, Membership-dependent stability conditions for type-1 and interval type-2 T-S fuzzy systems. Fuzzy Sets and Systems 356 (2019) 44-62.
[36] M. Wang, G. Feng, H. C. Yan, J. B. Qiu, and H. Zhang, Membership-function-dependent fault detection filtering design for interval type-2 T-S fuzzy systems in finite frequency domain. IEEE Transactions on Fuzzy Systems 29 (2021) 2760-2773.
[37] L. X. Zhang and J. Lam, Necessary and sufficient conditions for analysis and synthesis of Markov jump linear systems with incomplete transition descriptions. IEEE Transactions on Automatic Control 55 (2010) 1695-1701.
[38] S. L. Dong, Z.-G. Wu, H. Y. Su, P. Shi, and H. R. Karimi, Asynchronous control of continuous-time nonlinear Markov jump systems subject to strict dissipativity. IEEE Transactions on Automatic Control 64 (2019) 1250-1256.
[39] A. Seuret and F. Gouaisbaut, Wirtinger-based integral inequality: Application to time-delay systems. Automatica 49 (2013) 2860-2866.
[40] P. G. Park, W. I. Lee, and S. Y. Lee, Auxiliary function-based integral inequalities for quadratic functions and their applications to time-delay systems. Journal of the Franklin Institute 352 (2015) 1378-1396.

Yinghong Zhao received the M.S. degree in mathematics from Yanshan University, Qinhuangdao, China, in 2022. She is currently working toward the Ph.D. degree in control science and engineering with the School of Artificial Intelligence, Hebei University of Technology, Tianjin, China.

Her current research interests include T-S fuzzy systems, Markov jump systems, and control system theory.

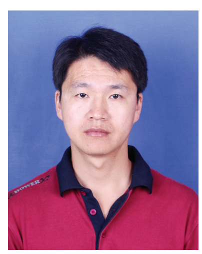

Likui Wang received the B.S degree in applied mathematics from Tangshan Normal University, Tangshan, China, in 2003, the M.S. degree in operations research and cybernetics from Yanshan University, Qinhuangdao, China, in 2005, and the Ph.D. degree in control theory and control engineering from the Dalian University of Technology, Dalian, China, in 2009.

He is currently a Professor with the School of Artificial Intelligence, Hebei University of Technology, Tianjin, China. His current research interests include fuzzy control theory, time-delay systems.

Xiangpeng Xie (Member, IEEE) received the B.S. and Ph.D. degrees in engineering from Northeastern University, Shenyang, China, in 2004 and 2010, respectively.

From 2010 to 2014, he was a Senior Engineer with Metallurgical Corporation of China Ltd., Beijing, China. He is currently a Professor with the Institute of Advanced Technology, Nanjing University of Posts and Telecommunications, Nanjing, China. His research interests include fuzzy modeling and control synthesis, state estimations, optimization in process industries, and intelligent optimization algorithms.

Prof. Xie serves as an Associate Editor for the International Journal of Control, Automation, and Systems and the International Journal of Fuzzy Systems.

Jiayue Hou is currently working toward a Bachelor's Degree in Network Engineering from Nanjing University of Posts and Telecommunications, Nanjing, China. Her research interests include automatic control, fuzzy modelling and posture estimation.

Hak-Keung Lam (Fellow, IEEE) received the B.Eng. (Hons.) and Ph.D. degrees from the Department of Electronic and Information Engineering, The Hong Kong Polytechnic University, Hong Kong, in 1995 and 2000, respectively.

In 2000 and 2005, he worked with the Department of Electronic and Information Engineering, The Hong Kong Polytechnic University as a Postdoctoral Fellow and a Research Fellow, respectively. He joined as a Lecturer with King's College London, London, U.K., in 2005, where he is currently a Reader. He is a coeditor of two edited volumes and an author/coauthor of three monographs. His current research interests include intelligent control, computational intelligence, and machine learning.

Dr. Lam is an Associate Editor of IEEE TRANSACTIONS ON FUZZY SYSTEMS, IEEE TRANSACTIONS ON CIRCUITS AND SYSTEMS-PART II: EXPRESS BRIEFS, IET Control Theory and Applications, International Journal of Fuzzy Systems, Neurocomputing, and Nonlinear Dynamics; and a guest editor and on the editorial board for a number of international journals. He was named as a Highly Cited Researcher.